Supporting Information for:

Facile Phase Transfer of Gold Nanoparticles From Aqueous Solution to Organic Solvents with Thiolated Poly(ethylene glycol)

A. M. Alkilany, A. I. Bani Yaseen, J. Park, J. R. Eller and C. J. Murphy

Material and Methods. Chloroauric acid ($HAuCl_4.3H_2O$, 99.9%), sodium borohydride ($NaBH_4$, 99%), silver nitrate ($AgNO_3$, 99+%), cetyltrimethylammonium bromide (CTAB, 99%, Sigma Ultra), ascorbic acid (99+%), trisodium citrate, Poly(ethylene glycol) methylether thiol (PEG-SH, Mn=5000 Da), 1-Dodecanethiol (DDT, ≥98%) and Tetraoctylammonium bromide (TOAB, 98%) were obtained from Sigma-Aldrich and used as received. Poly(ethylene glycol) methylether thiol (PEG-SH, Mn=350, 1000, 20000 Da) and FITC-PEG-SH (5000 Da) were obtained from NanoCS Inc (Boston, USA) and used as is. PDI values of PEG-SH were in the range of 1.04-1.10 (supplier values). All solvents were obtained from VWR and used as received. All solutions were prepared with purified 18 MΩ water. Glassware was cleaned with aqua regia and rinsed thoroughly with 18 MΩ water.

Instrumentation. Absorption spectra were taken using a UV/VIS spectrophotometer (Spectrascan 80D, Biotech Eng., UK). Fluorescence spectra were taken using SLM-Aminco Model 8100 spectrofluorometer (Spectronic Instruments, Rochester, NY, USA). Samples were excited at 494 nm. Transmission electron microscopy (TEM) images were obtained with a Philips CM200 electron microscope operating at 120 kV attached to a peltier-cooled Tietz 2k x 2k CCD camera. TEM grids were prepared by dropcasting 10 μL of purified gold nanoparticle dispersions on lacey carbon coated copper TEM grids (400 mesh, Ted Pella Inc., Redding, CA), and allowing them to dry in air. XPS measurements were made using a Kratos Axis Ultra photoelectron spectrometer (Kratos Analytical, Inc., Manchester, UK) using monochromatic Al Ka radiation (1486.6 eV). High-resolution spectra were collected with a pass energy of 20 eV from a 0.7 mm x 0.3 mm area. The binding energy scale was referenced to the adventitious C 1s signal at 285 eV. Samples for XPS were prepared by dropcast 10 μL of purified solution of GNPs on gold (0.01 nM) coated glass slide and let it evaporate at room temperature.

Synthesis of citrate-capped gold nanoparticles (Cit-GNPs)

Citrate-capped gold nanoparticles were synthesized using Frens method.[1] An aqueous solution of 0.25 mM $HAuCl_4$, 100 mL, was heated in a conical flask and brought to boiling. To the boiling solution, 3.0 mL of an aqueous solution of 1% (w/w) sodium citrate was added. The heating was maintained until a deep ruby red colour appeared (10 minutes), indicating the formation of gold nanoparticles (average diameter = 12.2 ± 1.4 nm).

Synthesis of gold nanoparticles using the hydroquinone method

A seed-mediated protocol detailed elsewhere was employed to prepare large GNPs using hydroquinone as a reducing agent.[2] First, seeds were prepared by boiling an aqueous gold solution (0.25 mM, 30 mL) in presence of sodium citrate (0.03% w/v) until a red colour developed indicating the formation of small gold nanoparticles. Second, the prepared seeds were used to grow larger nanoparticles by seeding an aqueous solution of seeds, gold salt, sodium citrate and hydroquinone as per the table below:

Vial number	DI Water, mL	Seed (As prepared), µL	Gold solution ($HAuCl_4$) (1% w/v), µL	Sodium citrate solution (1% w/v), µL	Hydroquinone solution (0.03 M), µL
1	9.28	500	100	22	100
2	9.43	350	100	22	100
3	9.63	150	100	22	100
4	9.73	50	100	22	100
5	9.75	25	100	22	100
6	9.77	10	100	22	100

Table S1. Synthesis of large GNP using the hydroquinone method. Added seed volume was varied to prepare GNP with various dimensions as per table S2.

Synthesis of CTAB-capped gold nanorods

Gold nanorods were prepared using a silver-assisted seeded-mediated method in the presence of the cationic surfactant cetyltrimethylammonium bromide (CTAB), as previously described.[3] CTAB-stabilized gold spheres (seed particles) were first prepared by sodium borohydride reduction. A solution of 2.5×10^{-4} M $HAuCl_4$ was prepared in 0.1 M aqueous CTAB in a 50 mL centrifuge tube. $NaBH_4$ (600 μL, of a 10 mM stock solution) was added to the gold/CTAB solution (10 mL) with vigorous stirring for 10 min. The resulting seed particles were then added to freshly prepared growth solutions. To prepare the gold nanorod growth solution, the following reagents were added (in the order described) to an aqua regia-cleaned Erlenmeyer flask: CTAB solution (95 mL of a 0.1 M stock solution), silver nitrate solution (0.1-1 mL of a 10 mM stock solution) to prepared GNR with various dimensions, and $HAuCl_4$ (5 mL of a 10 mM stock solution). An aqueous solution of ascorbic acid (0.55 mL of a 0.1 M stock solution) was then added with gentle mixing. Finally, the gold seed solution (0.12 mL) was added and mixed and left undisturbed overnight. The GNR solution was purified twice by centrifugation at 8000 rcf for 30 minutes to remove excess CTAB.

Typical phase transfer experiment

In a typical phase transfer experiment; PEG-SH (0.2 mg) is dissolved in 2.0 mL of dichloromethane (DCM). An aqueous solution of GNP (2.0) mL is added to the DCM phase followed by the addition of 2.0 mL of methanol (3.0 mL for nanorods) or other evaluated common solvent. Hand shaking is performed for few seconds to form an emulsion, which is not stable and the two layers separate rapidly with an efficient transfer of GNP from the aqueous phase (top) to the DCM phase (bottom). Addition of more methanol (up to 5.0 mL) followed by gentle shaking is required to concentrate GNP in the DCM phase. Addition of excess methanol resulted in the formation of a monophasic system, which can be disrupted to form biphasic layers by adding few drops of water. When nanoparticle's stability is concerned during the phase transfer reaction, PEG-SH can be added to the aqueous layer (i.e. GNPs solution) for 20 minutes prior the addition of the aqueous layer on the top of the DCM layer followed by the addition of methanol to induce phase transfer.

Determination of partition coefficient of FITC-PEG-SH between DCM and water

In a glass vial, 1.0 mg of FITC-PEG-SH was dissolved in 20.0 mL DCM and then purified water (20 mL) was added to form a biphasic extraction system, which was shake gently on a Belly Dancer® Laboratory Shaker (Stovall, NC, USA) for 24 hours. Sample was then centrifuged briefly at 500 rcf for 2 minutes to ensure complete phase separation. Fluorescence emission intensities were measured for water layers before and after extraction, using fluorescence spectrophotometer. Partition coefficient was determined by the following equation:

$$K_{DCM\ /\ water} = \frac{(F_{initial} - F_{extracted})}{F_{extracted}}$$

where, F_{nitial} is the fluorescence intensity of the water layer prior to extraction and $F_{extracted}$ is the fluorescence intensity of the same aqueous layer after extraction. Dynamic range of a calibration curve for FITC-PEG-SH in water was used to determine the proper dilution prior to spectra recording.

Evidence for the presence of PEG-SH on GNPs

X-ray photoelectron spectroscopy (XPS) before and after transfer was employed to confirm the presence of PEG-SH shell after phase transfer on the nanoparticle's surface. XPS spectra for purified GNRs before transfer (Fig. S1a) shows a clear peak of N1S (400.2 eV) which is absent in the spectra obtained for GNRs after phase transfer in agreement with CTAB displacement by PEG-SH (Fig. S1b). Moreover, absence of peaks in the thiol region for GNRs before transfer and the presence of S2P peak (161.3 eV) for GNRs after transfer, which support the presence of thiol moieties and thus CTAB displacement by PEG-SH after phase transfer. Samples were purified carefully by three rounds of centrifugation at 8000 rcf for 20 minutes followed by dialysis (MWCO 100K) for 48 hours against purified water.

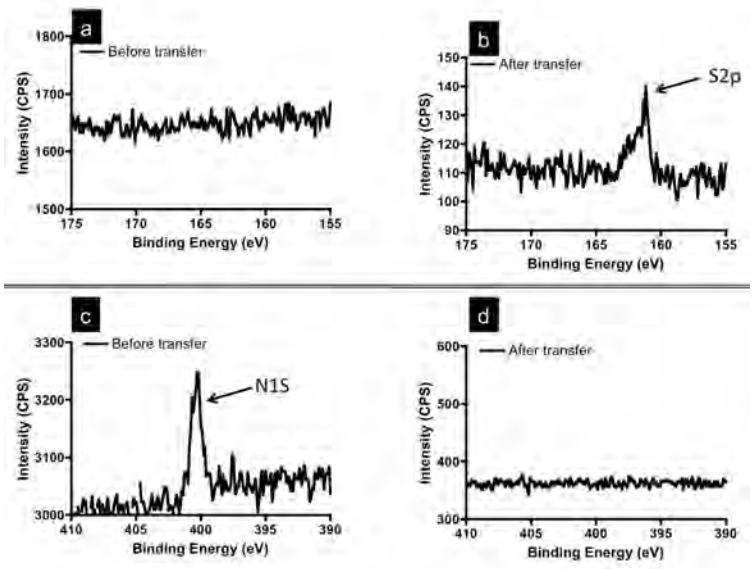

Fig. S1 X-ray photoelectron spectra of CTAB-GNRs before (a&c) and after (b &d) phase transfer. Upper panel contains spectra of thiol (S2p) where the lower panel shows spectra of nitrogen (N1S).

Another evidence of the presence of PEG-SH on the surface of GNRs after transfer is the extremely different solubility of GNRs in organic solvents such as

acetone. While typical PEG-GNRs have excellent solubility in water and organic solvents, CTAB-GNRs are known to have excellent aqueous solubility and poor resuspendibility in organic solvents. DCM layers with transferred GNRs were dried and the brownish residue was resuspended with water to yield a typical brown solution and UV-vis spectra. Both aqueous solutions of CTAB-GNRs and transferred GNRs were dried at 40 ^{o}C for 24 hours and then resuspended in DCM. Figure S2 shows typical UV-vis spectra of CTAB-GNRs in water before transfer as a control spectra shape and the spectra of CTAB-GNRs and transferred -GNRs as resuspended in DCM. CTAB-GNRs did not dissolve in DCM under aggressive sonication and their spectrum broadened significantly as per figure S2. However, dried transferred-GNRs were readily soluble in DCM upon mixing and they have typical UV-vis spectra with a shift in the longitudinal LSPR peak to higher wavelength due to the higher refractive index of DCM compared to water. The solubility of transferred GNRs in DCM and in water and also in a wide range of organic solvents (Fig. S9) support the presence of PEG shell at the surface of GNRs.

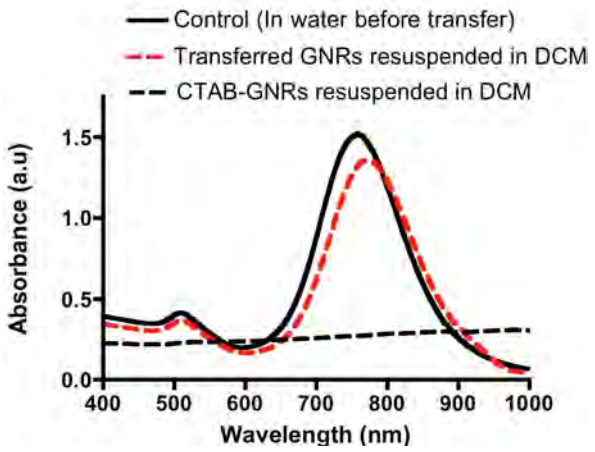

Fig. S2 UV-vis spectra of CTAB-GNRs in water before phase transfer (solid black line) and in DCM after phase transfer (red dashed line). Black dashed line represents CTAB-GNRs as dried from water and resuspended in DCM without phase transfer (black dashed line).

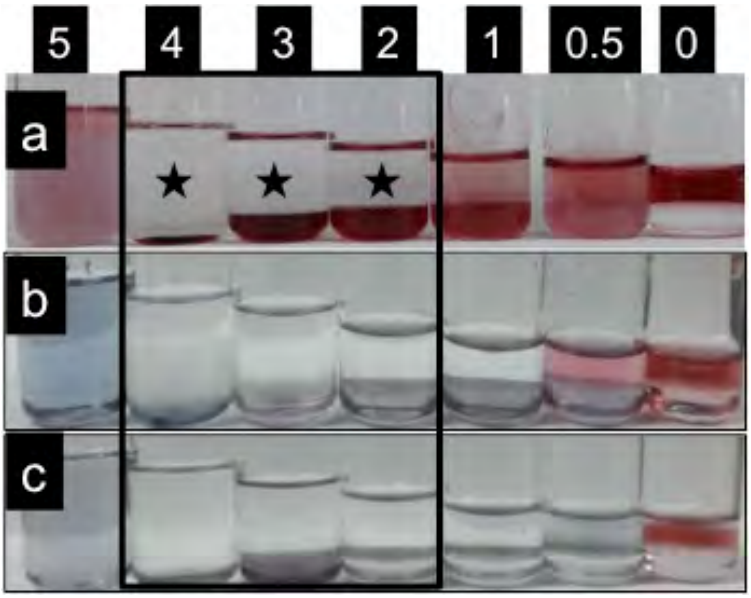

Fig. S3 Phase transfer of citrate-capped GNPs in water (2.0 mL) to DCM (2.0 mL) containing either: (a) PEG-SH, (b), DDT, or (c) TOAB. In all cases, the volume of methanol added was varied (0.5-5 mL as labelled). In the presence of PEG-SH, efficient phase transfer was observed in vials with the star symbol. In the presence of DDT and TOAB severe irreversible aggregation and nanoparticle assembly at the liquid-liquid interface was observed. Upon the addition of 5.0 mL (in all panels), single-phase system was observed.

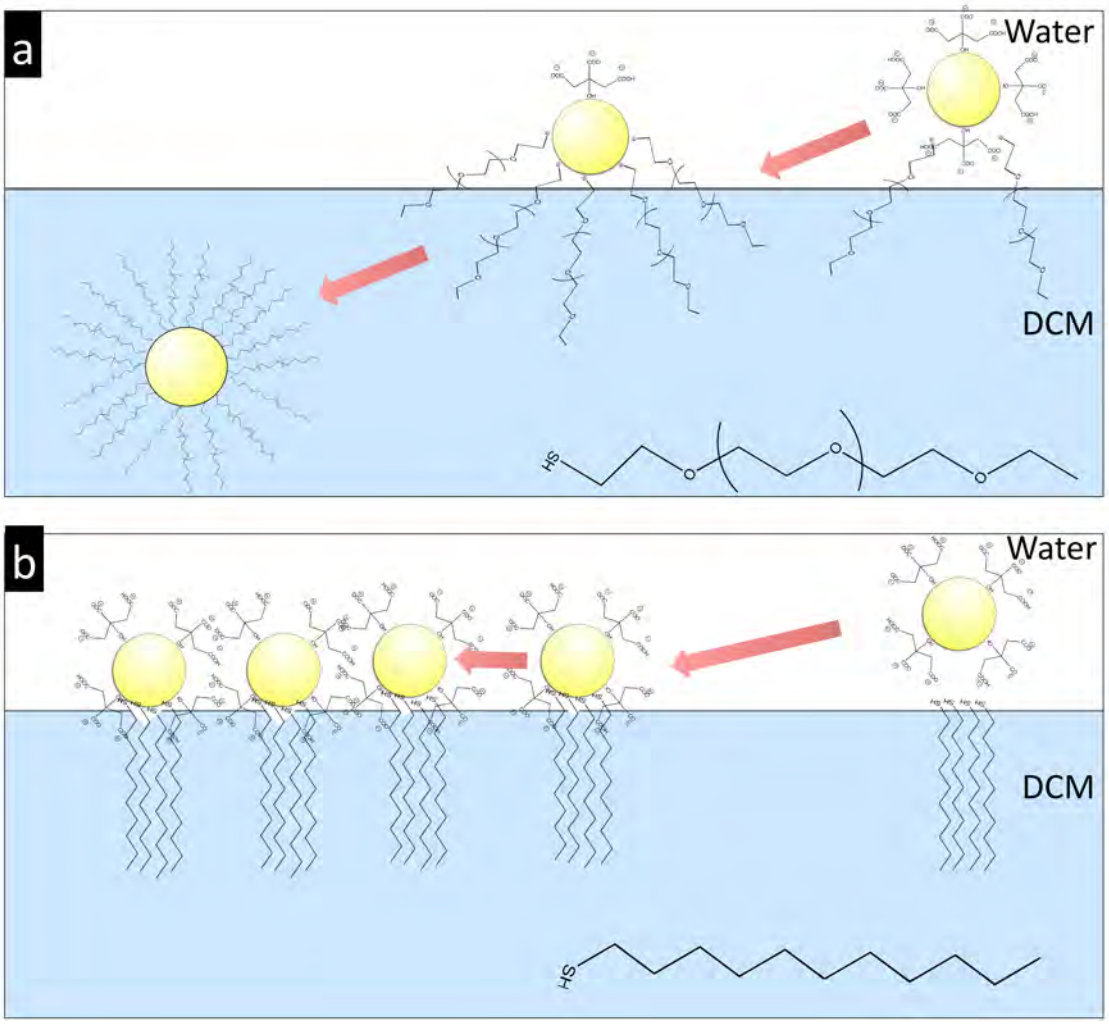

Fig. S4 Proposed explanation for a successful phase transfer using PEG-SH versus aggregation at the liquid-liquid interface when DDT was used as a phase transfer agent. (a) The excellent solubility of PEG-SH in both water and DCM and the dual properties of PEG molecules as both a hydrophilic and a hydrophobic molecule allow it to rapidly cover the nanoparticle's surface in both water and DCM resulting in efficient phase transfer without nanoparticle aggregation. In the case of highly hydrophobic phase transfer agent as DDT, nanoparticles will be capped partially in the DCM layer, which induce assembly of nanoparticles at the liquid-liquid interface and aggregation due to attractive forces between GNP at the interface as in (b). Molecular structures in the figure are used for representation and not to scale.

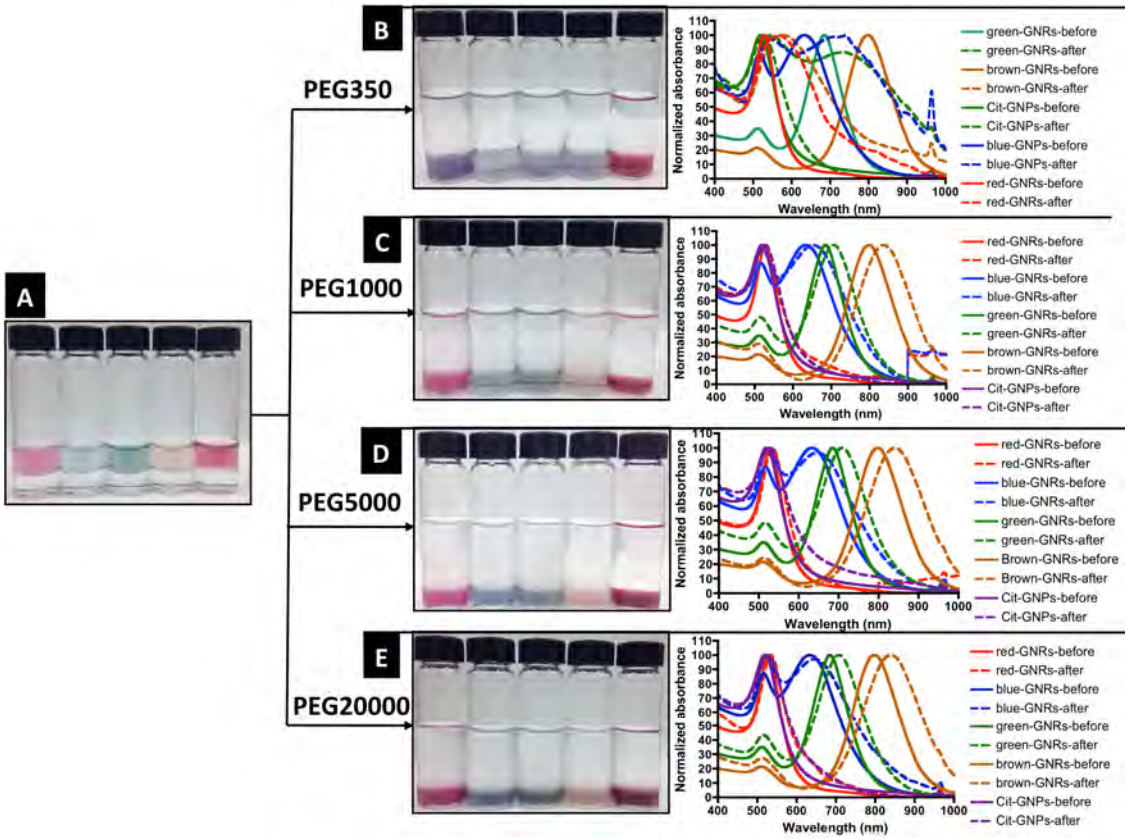

Fig. S5 Phase transfer of 2.0 mL of CTAB-capped gold nanorods with various aspect ratio (vials 1-4) or citrate-capped GNPs in water (vial 5) to 2.0 mL dichloromethane with 2.0 mL methanol. A) biphasic systems before phase transfer (upper layers represent aqueous layers with gold nanoparticles). B-E represent photographs and UV-vis spectra of vials after phase transfer with PEG-SH with various molecular weights (as indicated on the figure). Nanoparticle dimensions are tabulated in Table S3 and Figure S14. Note that complete phase transfer of GNPs from water to dichloromethane without nanoparticle aggregation is achieved with all evaluated PEG-SH polymers except PEG350 (MW of 350 Da) as evident from a significant change in vial colour and broadening in the UV-vis spectra for the transferred nanoparticles.

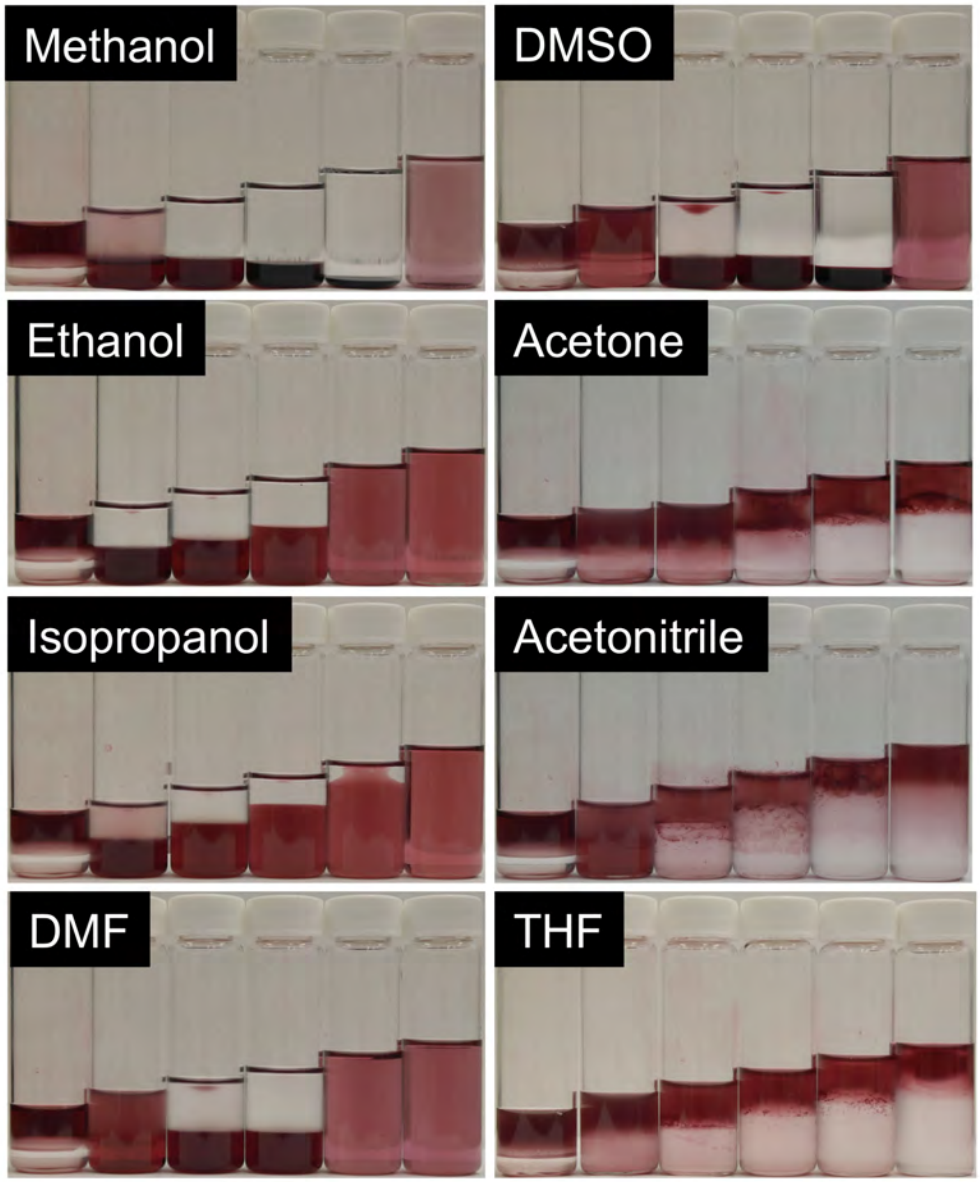

Fig. S6 Phase transfer of citrate-capped GNPs in water (2.0 mL) to DCM (2.0 mL) containing PEG-SH upon the addition of different common solvents as labelled. The added volume for each solvent was (0, 1, 2, 3, 4, 5 mL) from left to right in each image.

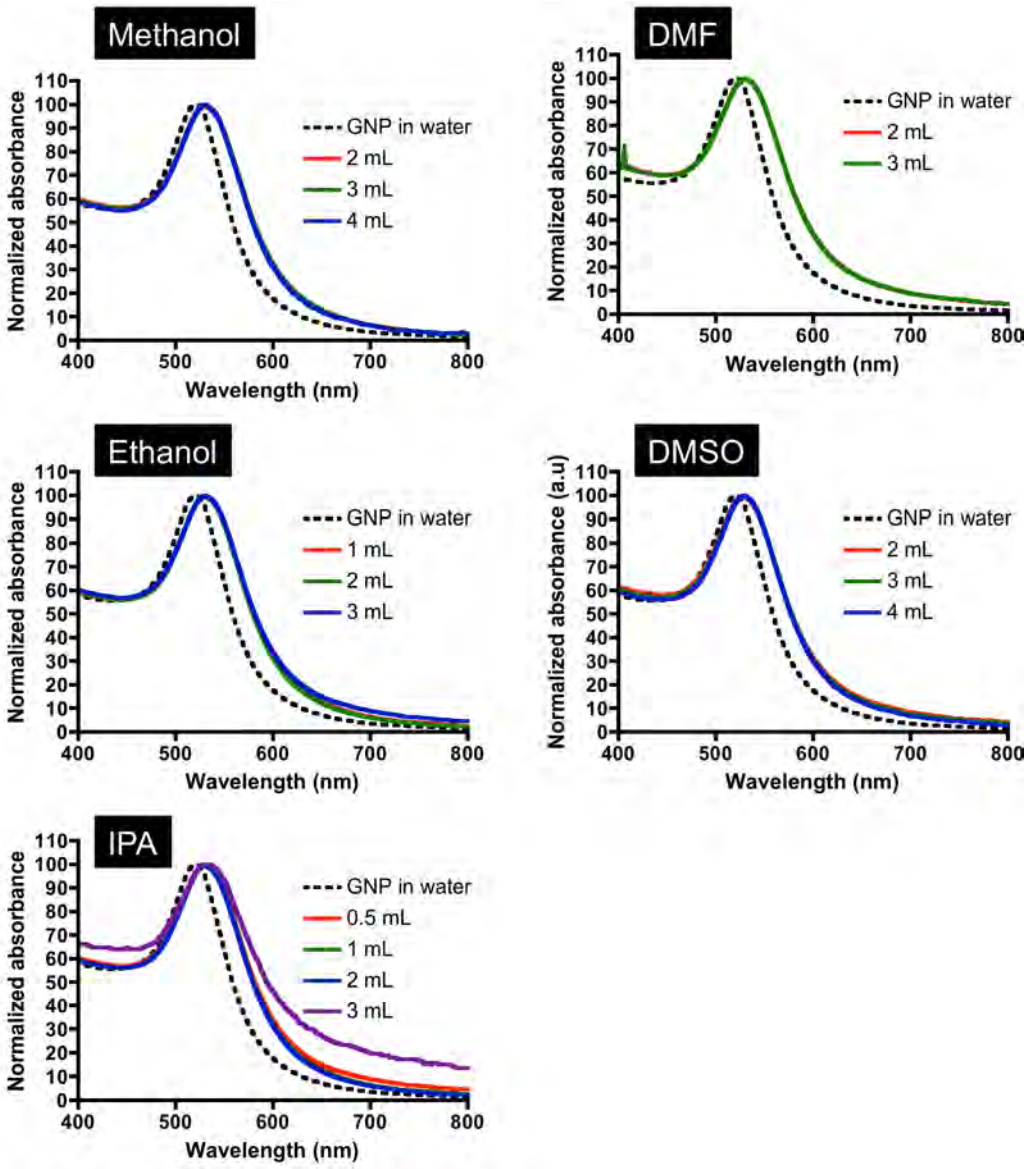

Fig. S7 UV-vis spectra of GNPs in water (dashed lines) versus in DCM layers after phase transfer with the addition of increasing volumes of different common solvents as indicated in the legends of each figure. Spectra were obtained only for the lower layers in the vials in Fig. S6, where complete phase transfer was observed for all solvents.

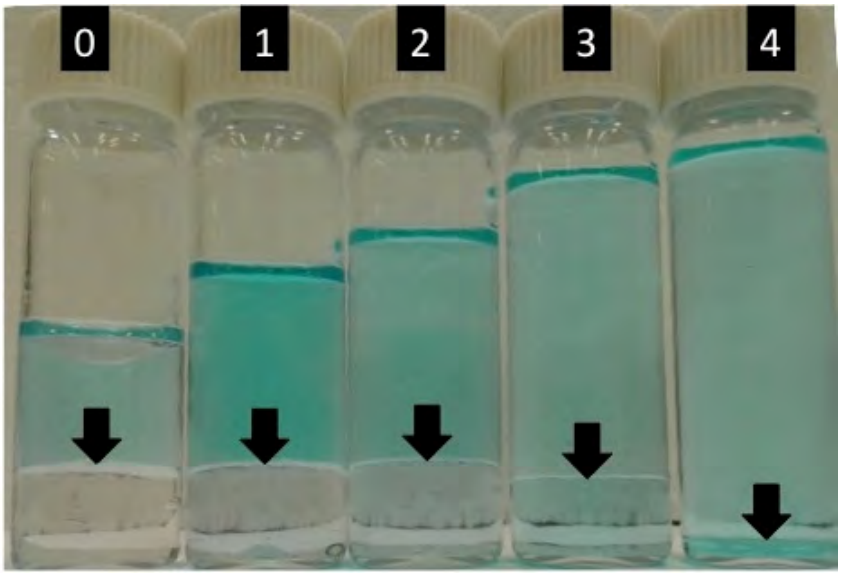

Fig. S8 Biphasic system of water-DCM systems upon the addition of methanol as labelled (in mL). After all systems reached equilibrium for phase separation, a drop of methylene blue solution (1% w/w) was added to each vial to visualize the liquid-liquid interface. In the absence of methylene blue it is hard to see the interface in the picture. Arrows show the liquid-liquid interface and the size of organic layers as function of methanol volume.

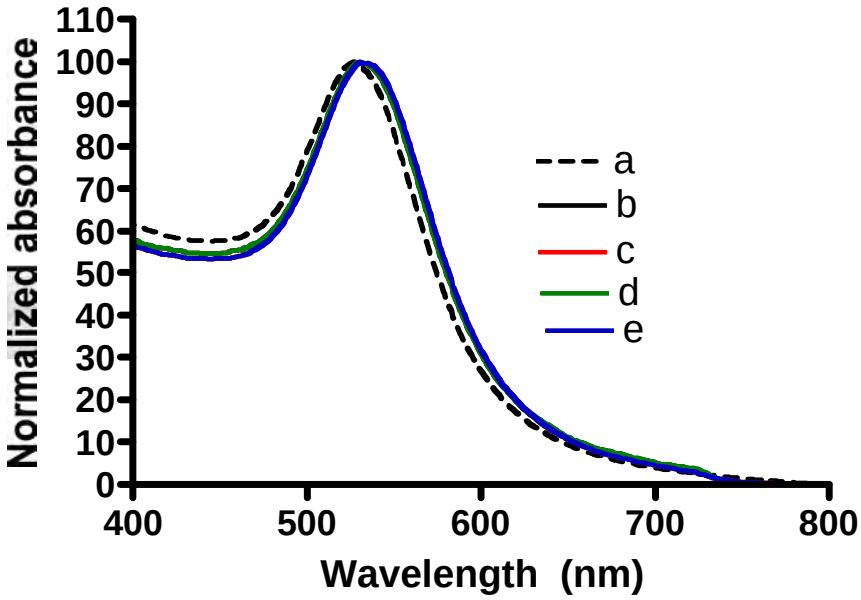

Fig. S9 Scale-up phase transfer corresponds to Fig.4: a) UV-vis spectra of citrate-capped GNPs in upper aqueous phase (before transfer, dashed line) versus in DCM layer after phase transfer with the addition of increasing volumes of methanol (in mL): b (150), c (225); d (300); e (350). Spectra were obtained for upper layer in Fig. 4a and lower layers for Fig. 4b-e.

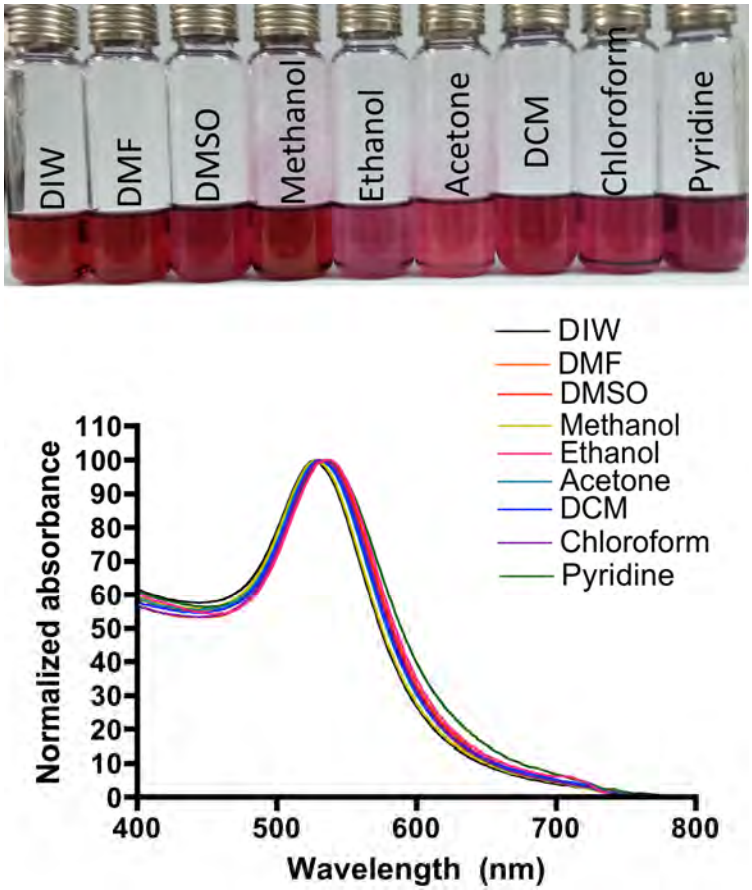

Fig. S10 Photographs and UV-vis spectra of phase transferred GNPs to DCM, using PEG-SH as a capping agent, followed by drying and re-suspension in different solvents as labelled.

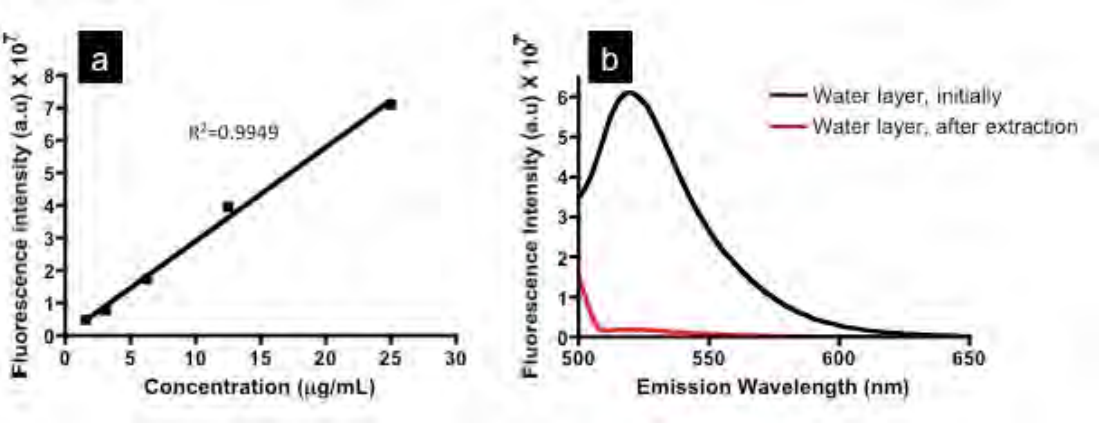

Fig. S11 Determination of the partition coefficient of FITC-PEG-SH between DCM and water as described in the experimental section. A) Calibration curve of FITC-PEG-SH in water. B) Fluorescence emission spectrum for FITC-PEG-SH in water layers, before and after extraction with DCM.

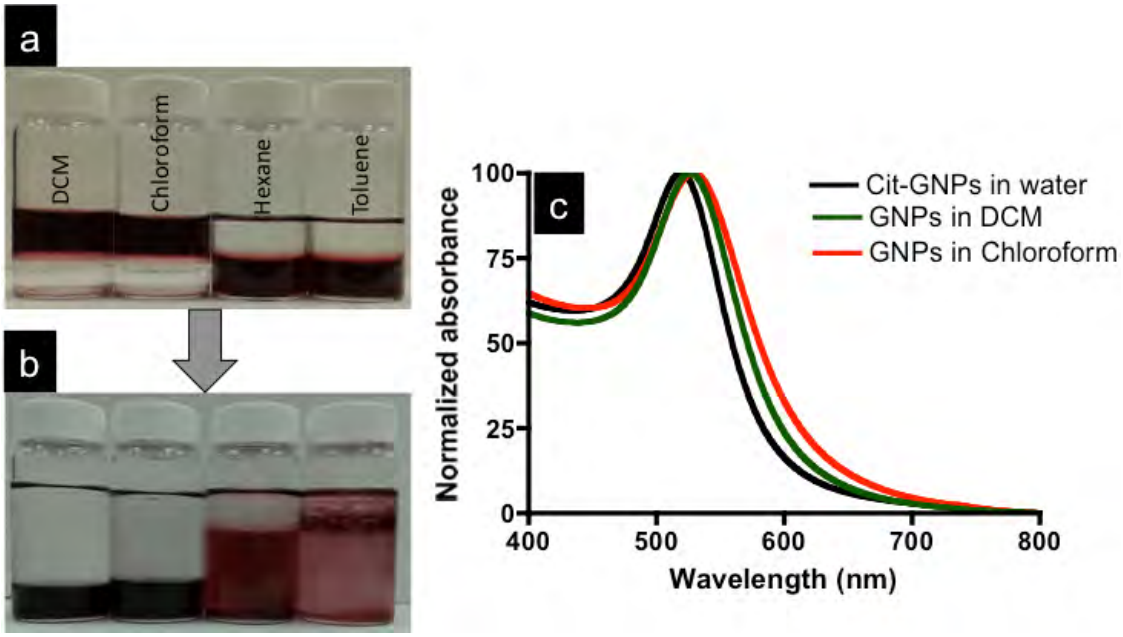

Fig. S12 Phase transfer of citrate-capped GNPs in water (5.0 mL) to various organic solvents before (a) and after (b) the addition of methanol to induce phase transfer. Note that PEG-GNPs only transferred efficiently to DCM and chloroform upon the addition of 7.5 mL methanol to each vial. UV-vis spectra of PEG-GNPs in DCM and chloroform have typical width and shape as compared to control spectra of the original cit-GNPs in water, indicating stable and evenly distributed nanoparticles in the organic layers.

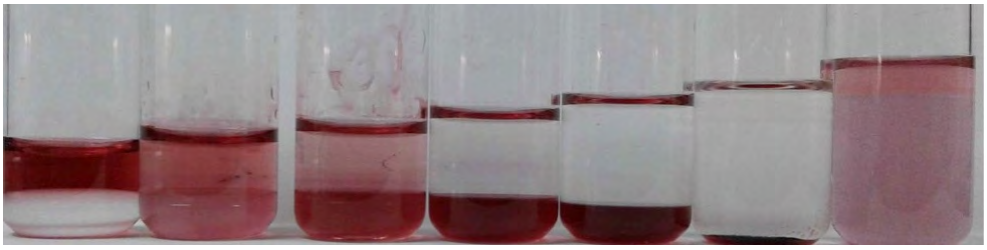

Fig. S13 Phase transfer of PEG-GNPs in water to DCM layer as function of the volume of added methanol (from left to right: 0, 0.5, 1, 2, 3, 4, 5 mL).

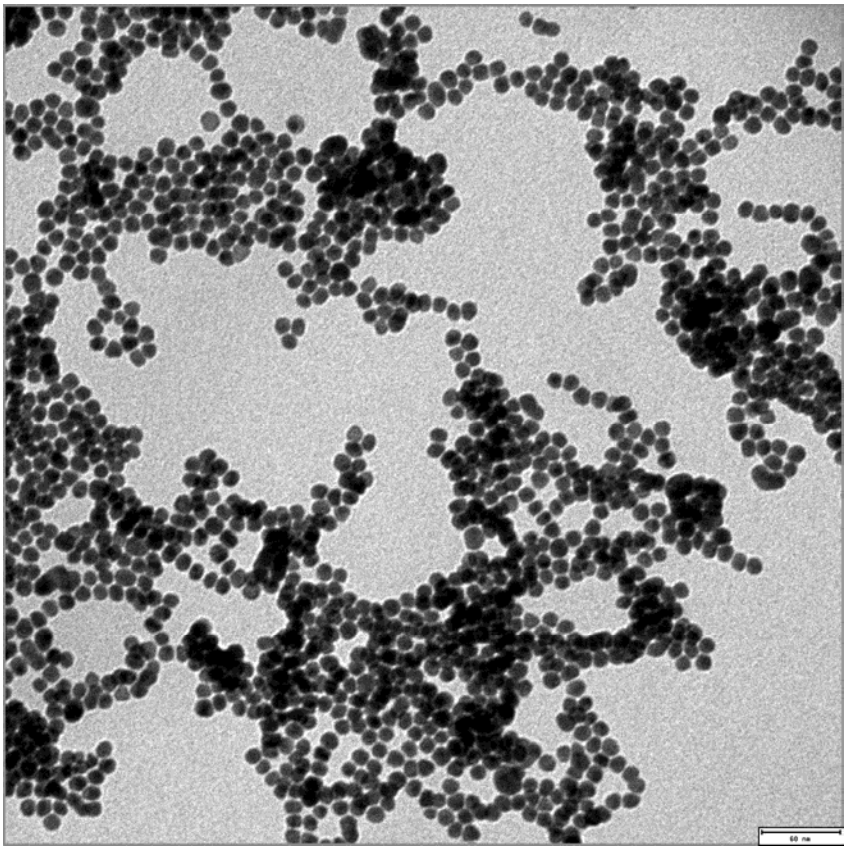

Fig. S14 TEM image of gold nanoparticles prepared using the Frens (citrate) method.[1] The particles in the image are from vial (a) in Fig.1. Mean particle size ±STD was 12.2±1.4 nm. Number of particles surveyed =100. Scale bar= 60 nm.

Vial number	Volume of added seeds solution (μL)	Mean sizes ± STD (nm)
1	500	23.1 ± 3.1
2	350	28.9 ± 3.5
3	150	35.7 ± 5.2
4	50	57.9 ± 10.7
5	25	77.5 ± 12.7
6	10	91.6 ± 14.1

Table S2. Size analysis of GNPs prepared using the hydroquinone method.[2] Added seed solution was varied to prepare GNPs with different sizes. "Vial number" corresponds to Fig. 3 from 1-6 as indicated. Number of particles surveyed per TEM image to calculate dimensions=100.

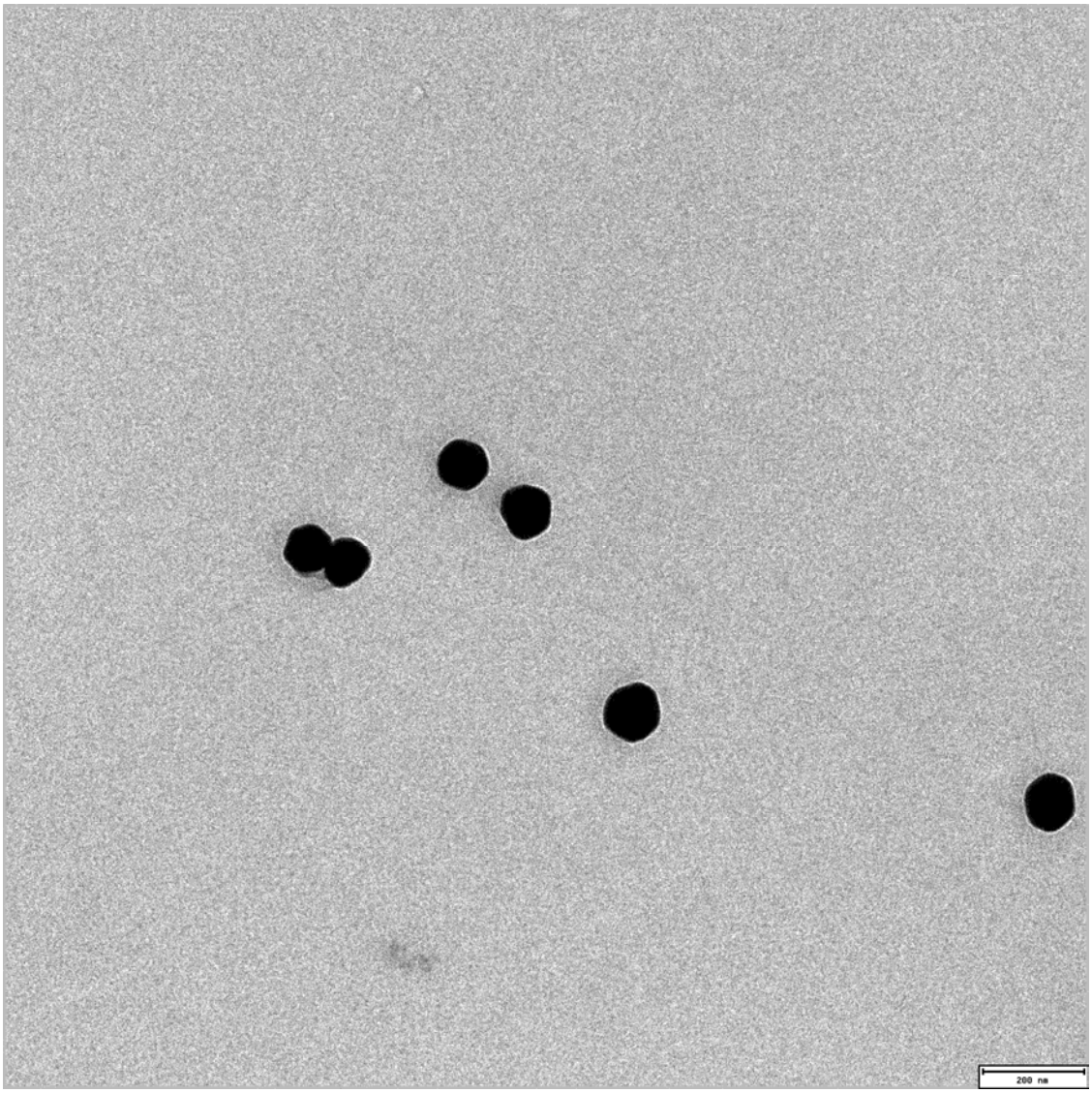

Fig. S15 TEM image of gold nanoparticles prepared using the hydroquinone method. The particles in the image are from vial 6 as shown in Fig. 3 and listed in table S2. Scale bar= 200 nm.

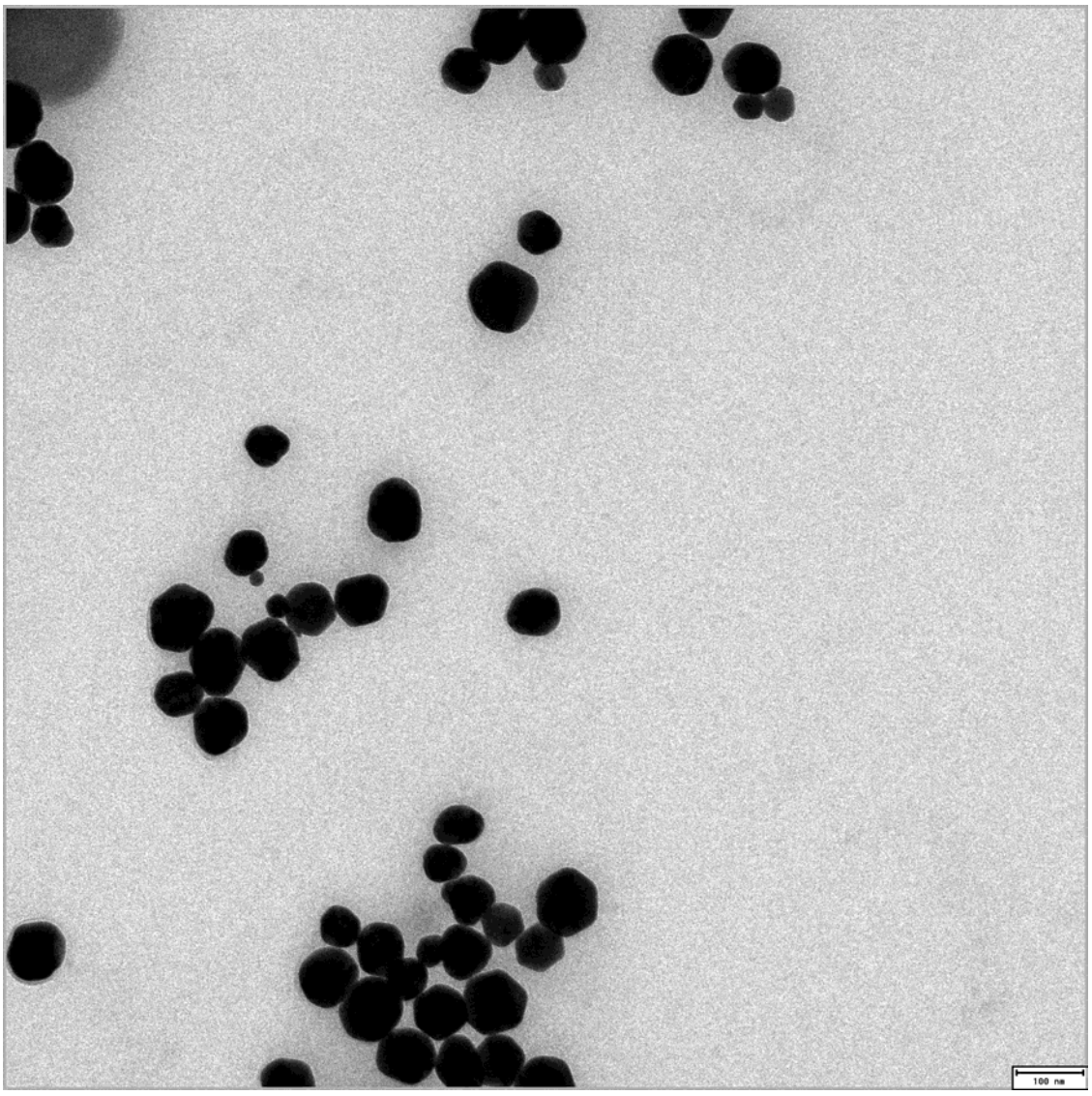

Fig. S16 TEM image of gold nanoparticles prepared using the hydroquinone method. The particles in the image are from vial 5 as shown in Fig. 3 and listed in table S2. Scale bar= 100 nm.

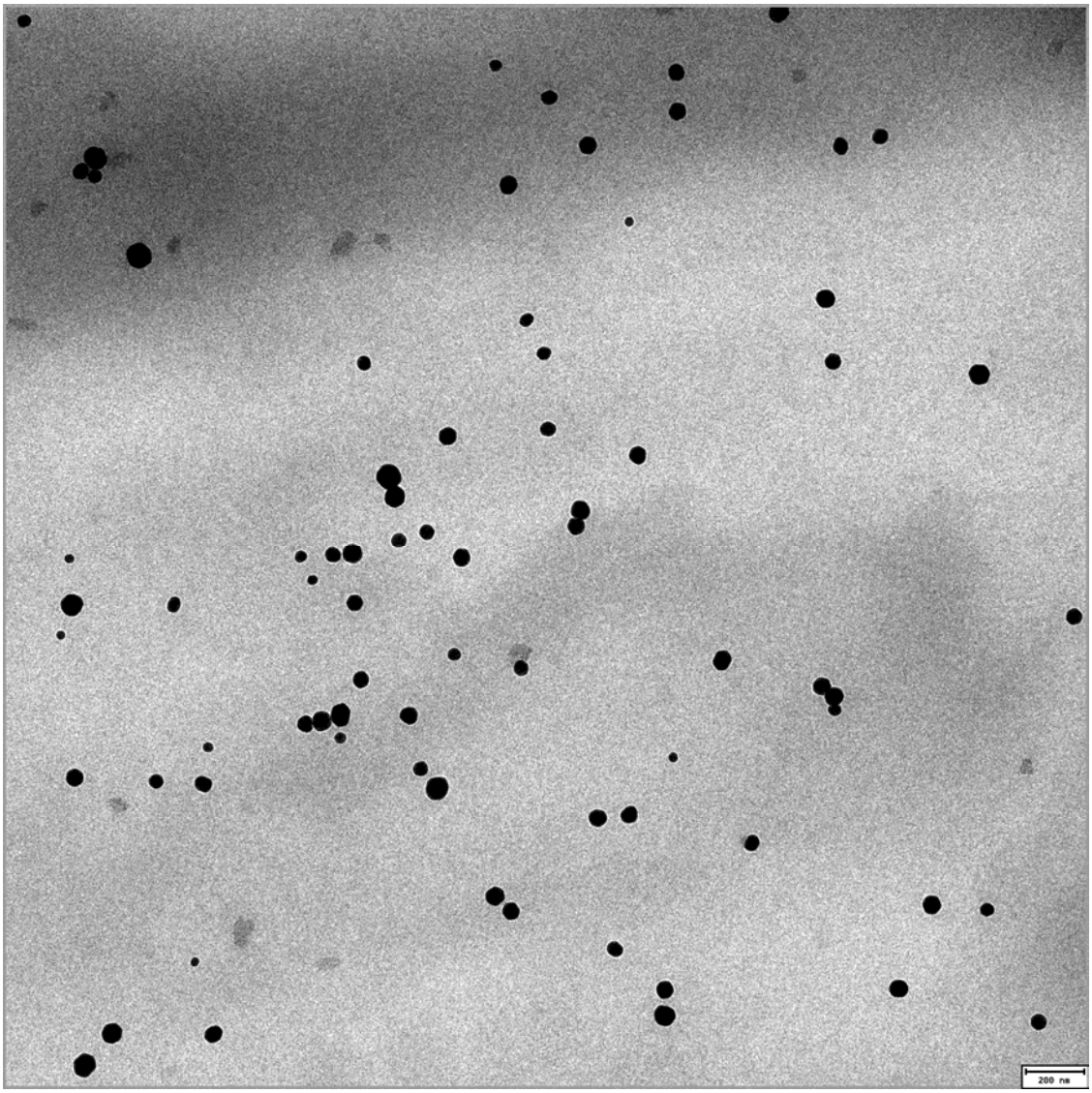

Fig. S17 TEM image of gold nanoparticles prepared using the hydroquinone method. The particles in the image are from vial 4 as shown in Fig. 3 and listed in table S2. Scale bar = 200 nm.

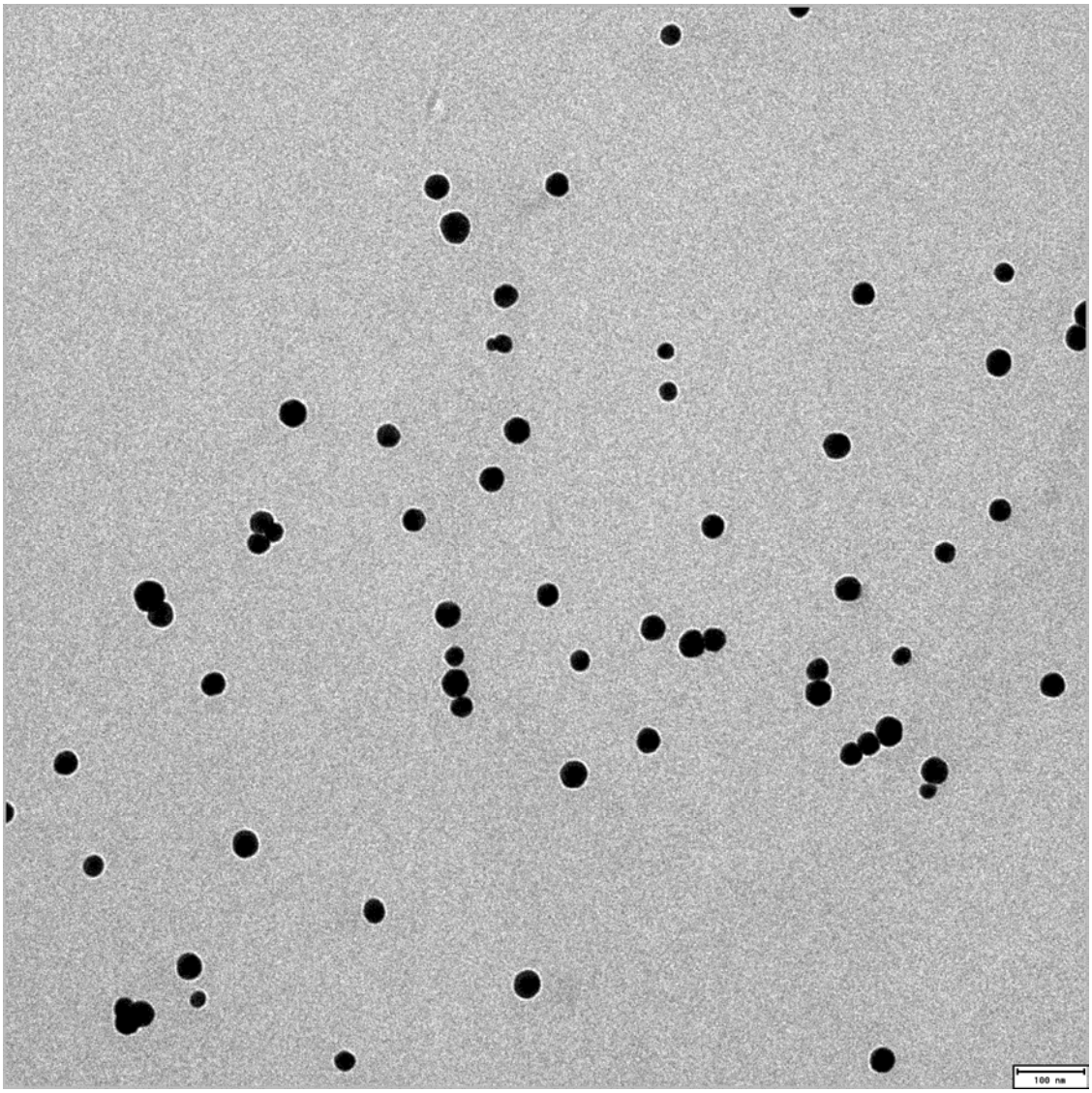

Fig. S18 TEM image of gold nanoparticles prepared using the hydroquinone method. The particles in the image are from vial 3 as shown in Fig. 3 and listed in table S2. Scale bar = 100 nm.

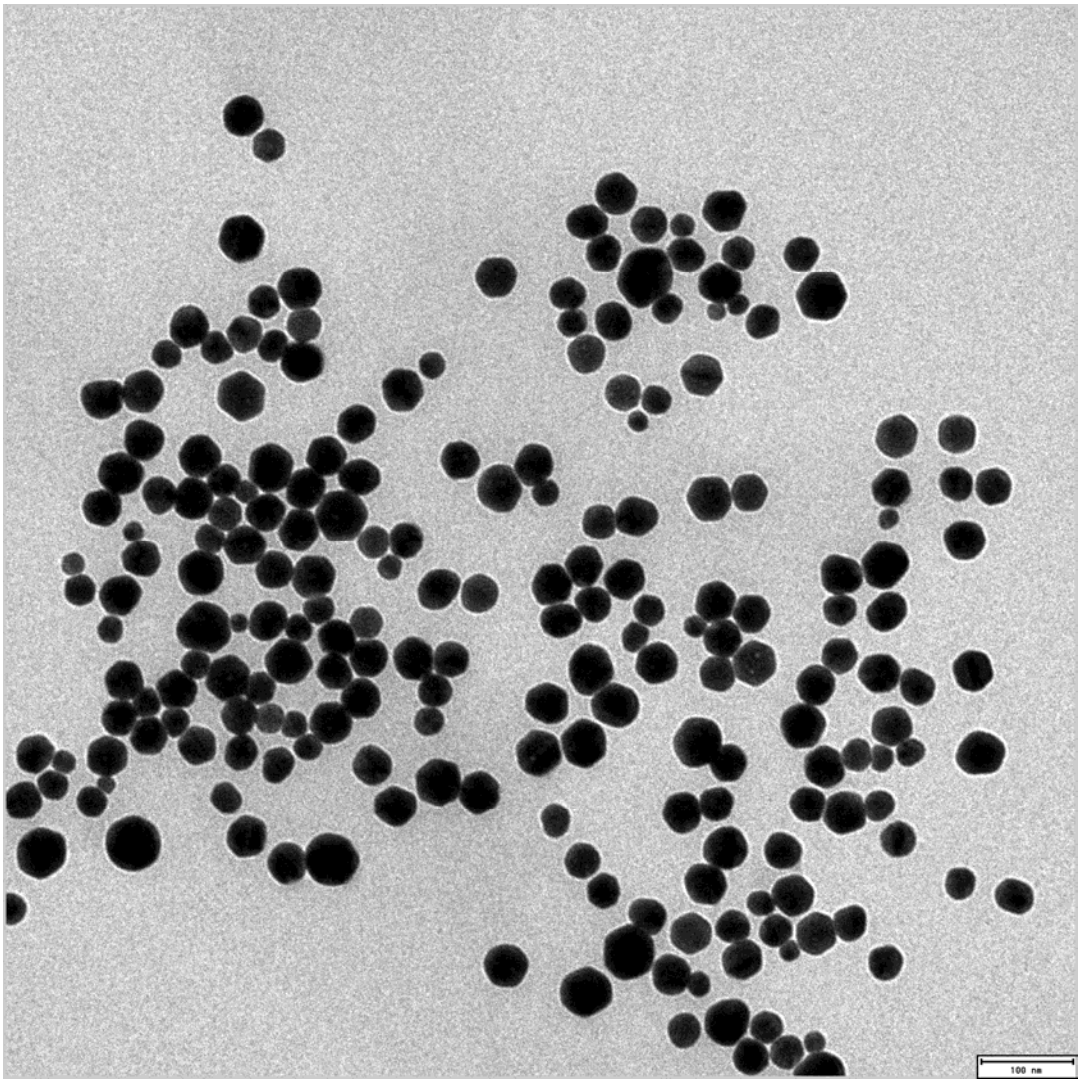

Fig. S19 TEM image of gold nanoparticles prepared using the hydroquinone method. The particles in the image are from vial 2 as shown in Fig. 3 and listed in table S2. Scale bar = 100 nm.

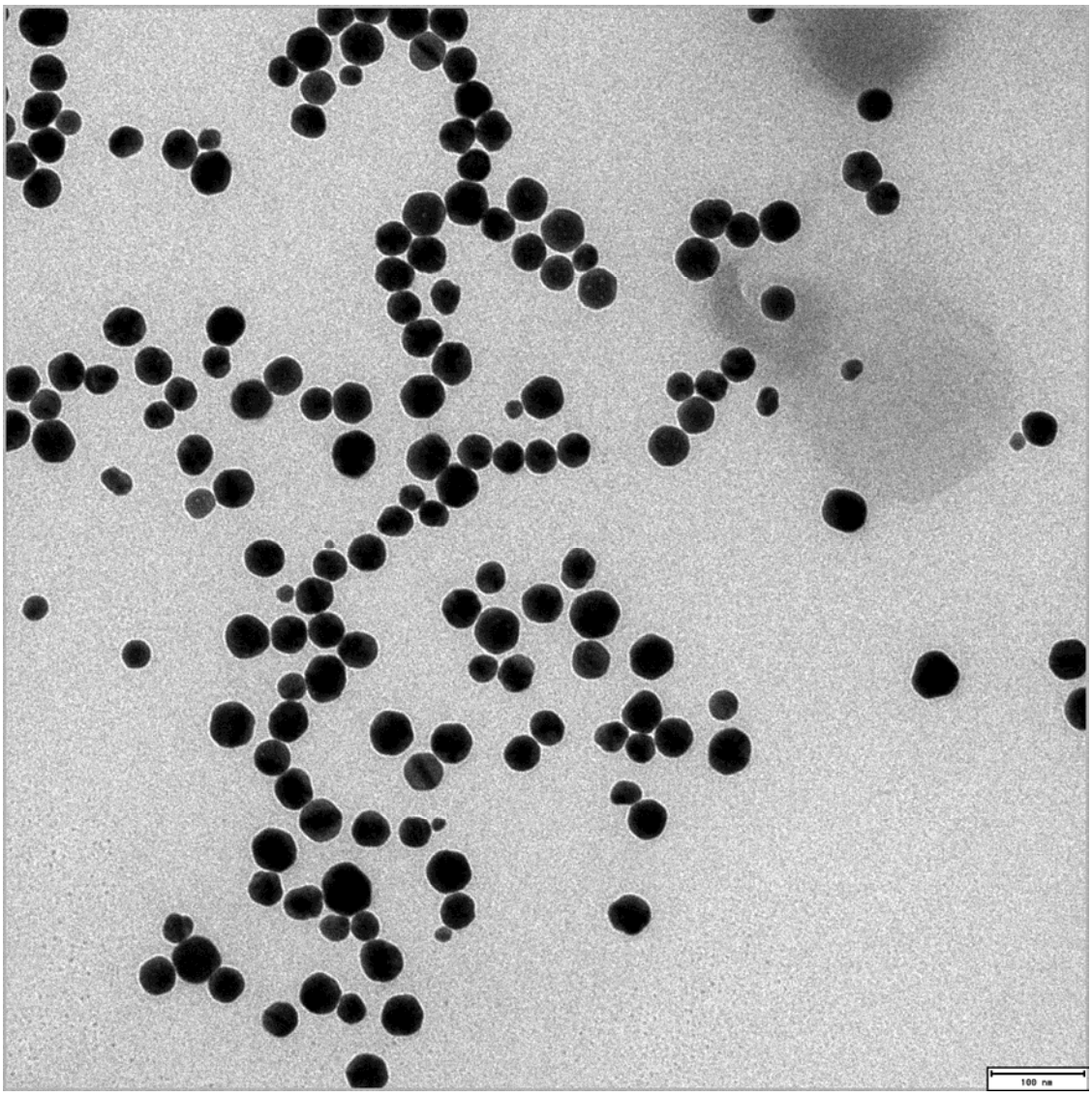

Fig. S20 TEM image of gold nanoparticles prepared using the hydroquinone method. The particles in the image are from vial 1 as shown in Fig. 3 and listed in table S2. Scale bar = 100 nm.

Vial number	Volume of $AgNO_3$ solution (uL)	Mean length ±STDV (nm)	Mean width ±STDV (nm)	Mean aspect ratio (length/width) ±STDV (nm)
7	10	31.1 ± 6.7	27.1 ± 5.6	1.2 ± 0.32
8	25	42.2 ± 8.0	18.3 ± 3.6	2.4 ± 0.7
9	50	47.5 ± 10.7	15.7 ± 3.0	3.1 ± 0.6
10	100	55.3 ± 6.9	16.1 ± 2.7	3.5 ± 0.6

Table S3. Size analysis (length, width and aspect ration) of gold nanorods prepared using the wet-chemical seed-mediated method.[3] "Vial number" corresponds to Fig. 3 from 1-4 as indicated. Number of particles surveyed per TEM image to calculate dimensions=100.

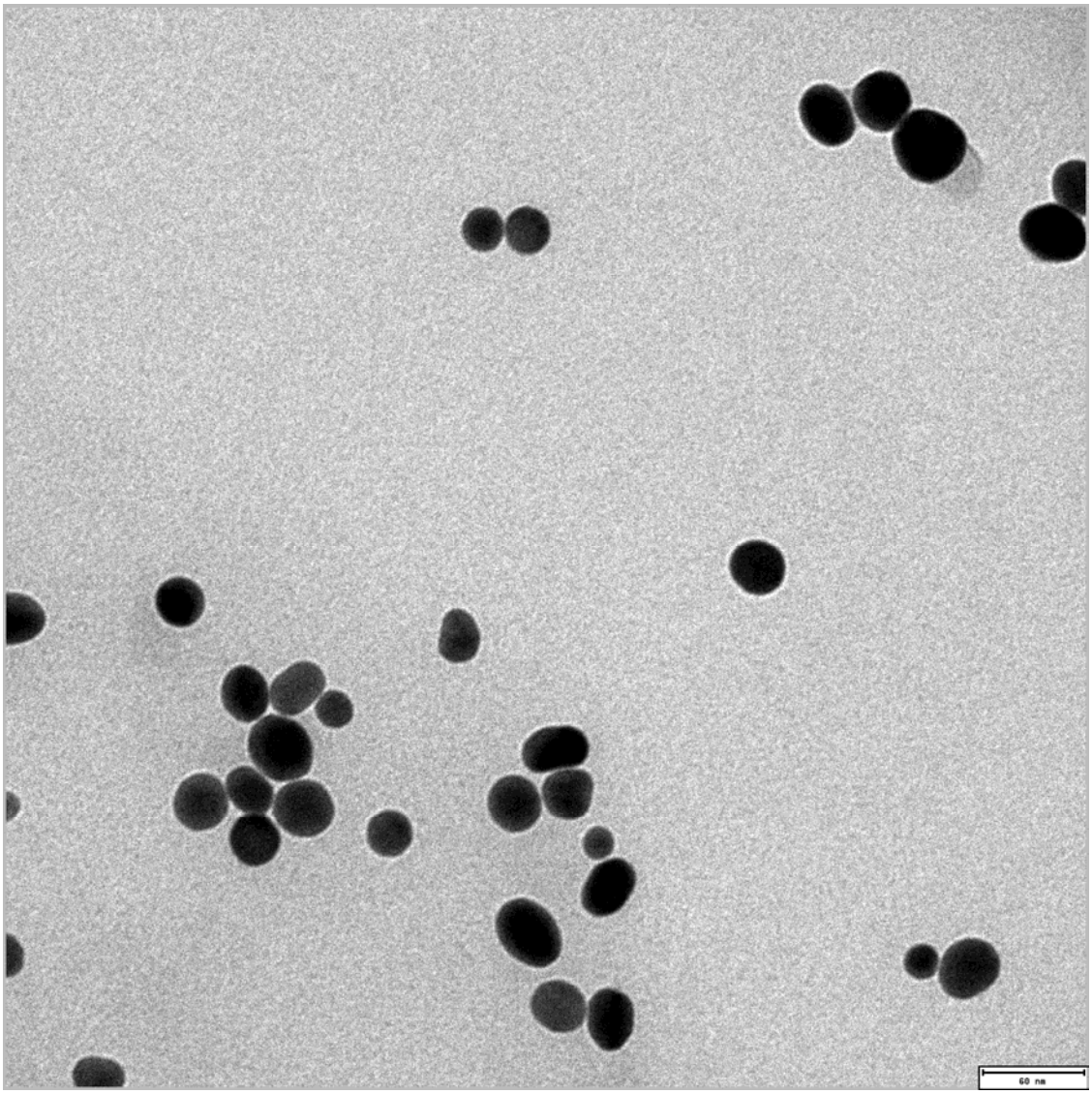

Fig. S21 TEM image of gold nanoparticles prepared using wet-chemical seed-mediated protocol as described in the experimental section. The particles in the image are from vial 7 as shown in Fig. 3 and listed in table S3. Scale bar = 60 nm.

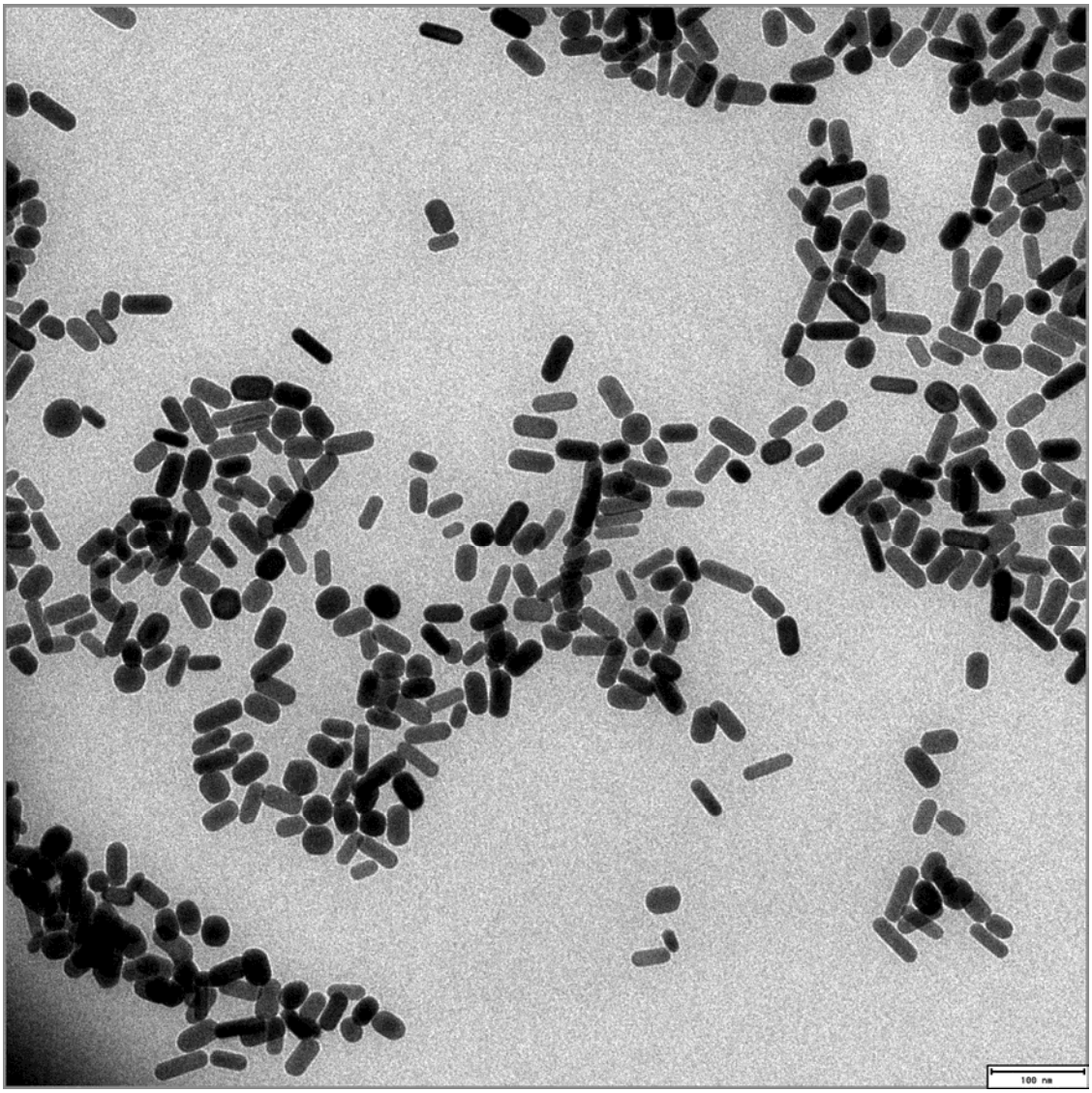

Fig. S22 TEM image of gold nanoparticles prepared using wet-chemical seed-mediated protocol as described in the experimental section. The particles in the image are from vial 8 as shown in Fig. 3 and listed in table S3. Scale bar = 100 nm.

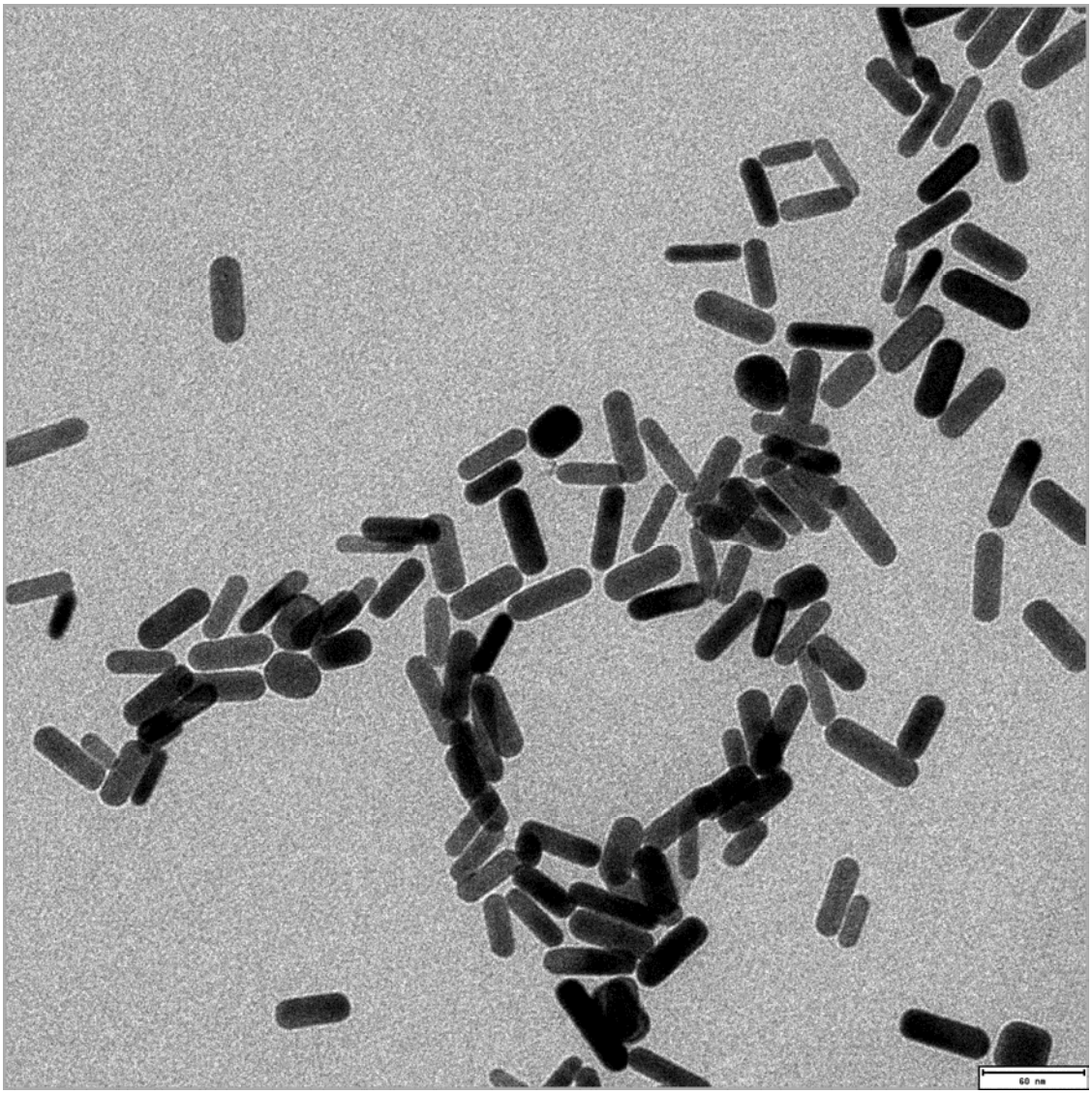

Fig. S23 TEM image of gold nanoparticles prepared using wet-chemical seed-mediated protocol as described in the experimental section. The particles were taken from vial 9 as shown in Fig. 3 and listed in table S3. Scale bar = 60 nm.

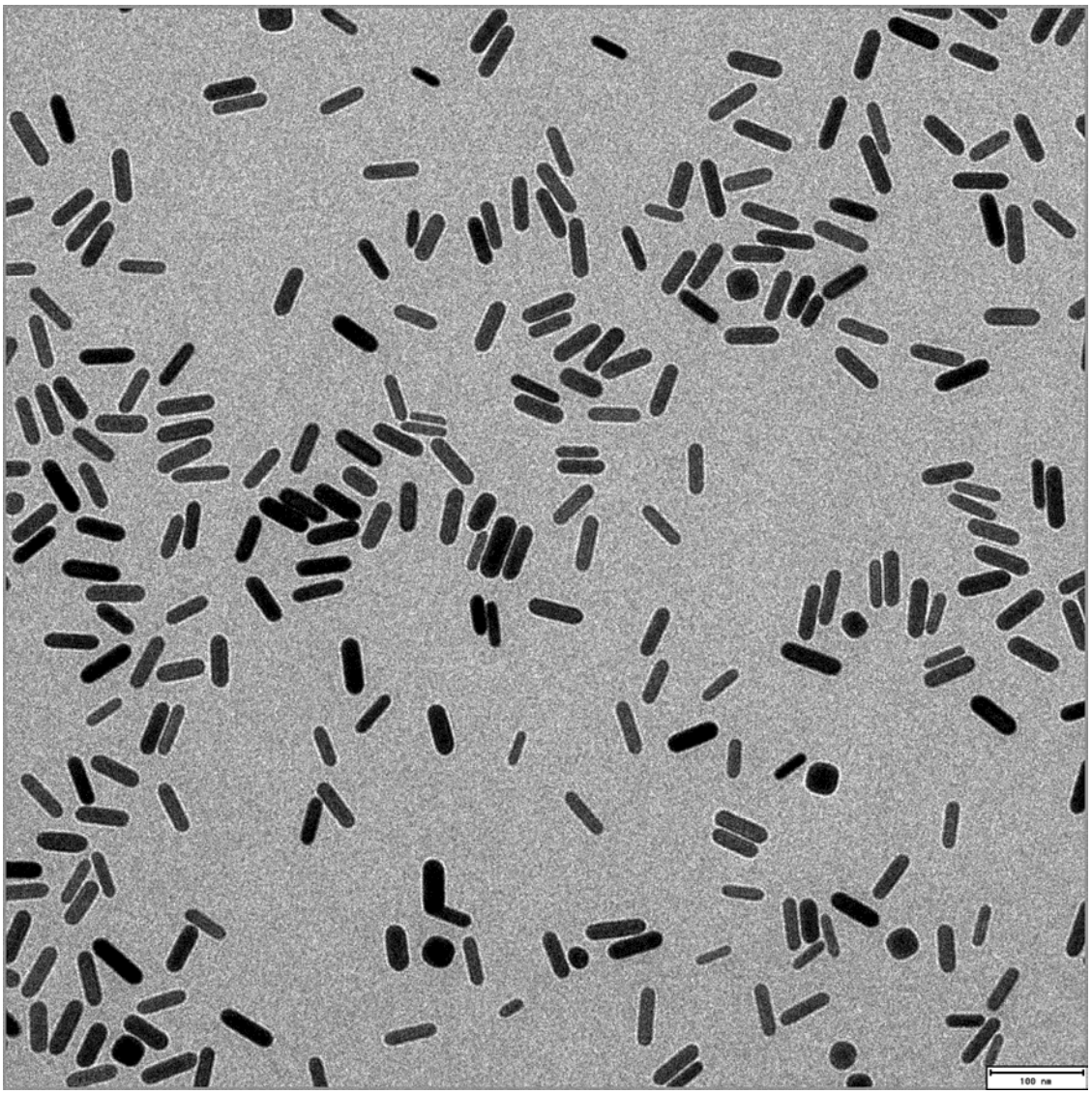

Fig. S24 TEM image of gold nanoparticles prepared using wet-chemical seed-mediated protocol as described in the experimental section. The particles in the image are from vial 10 as shown in Fig. 3 and listed in table S3. Scale bar = 100 nm.

References

1 G. Frens, *Nature*, 1973, **241**, 20.
2 S. D. Perrault and W. C. Chan, *J Am Chem Soc*, 2009, **131**, 17042.
3 T. K. Sau and C. J. Murphy, *Langmuir*, 2004, **20**, 6414.